



Characterization of sludge generated by electrocoagulation for the removal of heavy metals

Do-Gun Kim, Ronna Jane S. Palacios, Seok-Oh Ko*

Department of Civil Engineering, Kyung Hee University, 732, Deokyoungdaero, Giheung-gu, Yongin-si, Gyeonggi-do 446-701, Korea

Tel. +82 31 201 2999; Fax: +82 31 202 8805; email: soko@khu.ac.kr

Received 25 March 2013; Accepted 24 April 2013

ABSTRACT

In this work, heavy metal removal by electrocoagulation (EC) was evaluated, and the characteristics of the EC sludge were investigated to understand the behavior of heavy metals during EC. It was found that iron electrodes are superior to aluminum due to the negatively charged surface. Using iron electrodes, the removal rate of heavy metals increased as the current density increased and as the total initial heavy metal amount, either single or multiple heavy metals, decreased, suggesting that the efficiency is closely related to the floc amount. The X-ray diffraction (XRD) patterns showed that the chemical species in the EC sludge are different from those obtained by chemical equilibrium analysis, indicating that many electrochemical and chemical reactions occur during EC. The pH variation during EC and the XRD patterns of the sludge indicate that precipitation, adsorption, and chemical oxidation/reduction in the vicinity of the electrodes contribute much to Pb(II), Cd(II), and Cu(II) removal, respectively. In addition, the formation of Pb(OH)Cl, β -Cd₂(OH)₃Cl, and CuCl was found, indicating that chloride from the background electrolyte contributes to heavy metal precipitation. Scanning electron microscopy, transmission electron microscopy, and energy-dispersive X-ray spectroscopy analysis also showed that Pb(II) and Cu(II) are encapsulated by the flocs.

Keywords: Electrocoagulation; Heavy metal; Iron electrode; Sludge characteristics

1. Introduction

Heavy metals such as lead (Pb), actinium (Ac), copper (Cu), chromium (Cr), nickel (Ni), arsenic (As), mercury (Hg), and zinc (Zn) are commonly found in wastewater [1] and the soil-washing effluent from agricultural areas and firearm shooting ranges [2,3].

They exert adverse effects both on human and aquatic ecosystems because they are nonbiodegradable, highly toxic, and carcinogenic [1]. There are various heavy metal treatment technologies, such as, adsorption, ion exchange, chemical coagulation, and electrocoagulation (EC) [1,4]. Precipitation is the most widely used, although a large amount of sludge is produced that requires further treatment. Ion exchange is efficient

*Corresponding author.

Presented at the Fifth Annual International Conference on “Challenges in Environmental Science & Engineering—CESE 2012” Melbourne, Australia, 9–13 September 2012

but is costly and difficult to operate. Adsorption is also efficient but the adsorbent is costly and the spent adsorbent should be disposed of after detoxification. EC offers the great advantage of high efficiency, a fast reaction rate, versatility, simplicity, amenability to automation, cost-effectiveness, easy compact instrumentation, minimum use of chemicals, and ease of operation [5]. In addition, EC involves a variety of electrochemical and chemical mechanisms, demonstrating that EC can be applied for the removal of a wide variety of pollutants [6].

The performance of EC has been studied to demonstrate its high efficiency in the removal of heavy metals [6–10] and a good settlability and dewaterability of EC sludge [10]. However, the removal of heavy metals is affected much by the electrode materials used. Kumar et al. [7] found that the removal efficiencies for arsenic at a pH range of 6–8 were 99, 37, and 58% for iron (Fe), aluminum (Al), and titanium (Ti) electrodes, respectively. Yadav et al. [6], Nansu-Njiki et al. [8], and Kumarasinghe et al. [9] also reported different Hg, Cu, Cr, Zn, and Ni removal when different electrodes were used. In addition, the reaction mechanisms, which are involved in heavy metal removal during EC, have not yet been explored sufficiently, although many pollutants removal mechanisms of EC have been suggested. The mechanisms include the chemical oxidation and reduction, electrophoretic migration, aggregation due to charge neutralization, precipitation, adsorption onto metal hydroxides formed during EC, sweep coagulation, and electroflotation by O_2 and H_2 bubbles produced [5,11]. Especially, the sludge characteristics, which can provide valuable information on the removal mechanisms of heavy metals by EC, have not been investigated in depth. Irdemez et al. [12] showed that the precipitates produced during phosphate removal by EC using Al electrodes are $Al(OH)_3$ and $AlPO_4$. Golder et al. [13] reported that the EC sludge generated during Cr(III) removal using mild steel electrode is amorphous, but no clear speciation of the sludge was provided. Drouiche et al. [14] investigated the X-ray diffraction (XRD) pattern of F-treatment sludge by EC using Al electrodes; but no chemical substance, with which the fate and mechanism of F^- removal can be suggested, was identified.

Therefore, in this study, the efficiency of EC in removing Pb(II), Cd(II), and Cu(II) in synthetic solutions was firstly investigated. The effect of the electrode material, current density, and initial heavy metal concentration was explored. Then, the characteristics of sludge generated by EC using Fe electrodes were analyzed by XRD, scanning electron microscopy (SEM), transmission electron microscopy (TEM),

energy-dispersive X-ray spectroscopy (EDS), and a zeta potential analyzer to investigate the behavior of heavy metals and the coagulant.

2. Materials and methods

2.1. Electrocoagulation

Fe and Al electrodes, having dimensions of 25×150 mm (thickness 5 mm), were used at a distance of 4 mm. The electrodes were scrubbed with sand paper, soaked with 1% hydrochloric acid for 24 h, and rinsed with deionized water (DIW) several times to remove passivation such as that from iron oxides/hydroxides on the surface [5]. The heavy metal stock solutions were prepared with DIW at $1,000 \text{ mg L}^{-1}$ for each heavy metal by dissolving a suitable amount of $Pb(NO_3)_2$, $Cd(NO_3)_2$, or $Cu(NO_3)_2$ at pH 4.5. Batch EC experiments were carried out for 60 min in a 1-L beaker containing the solution of heavy metals and 1 g L^{-1} NaCl as the background electrolyte [13]. The electrodes were immersed into the solution, and the solution was agitated at 100 rpm with a mechanical stirrer and a Teflon-coated agitator. Electric current was applied immediately after starting agitation with a DC power supply (SI-30200A, CNG). The current density was varied from 7.5 to 20 A m^{-2} , and the initial heavy metal concentration was varied from 10 to 100 mg L^{-1} . A set of experiments was conducted with solutions containing Pb, Cd, and Cu together at 10, 50, or 100 mg L^{-1} of each heavy metal, so that the total heavy metal concentration was 30, 150, or 300 mg L^{-1} , respectively, to investigate their simultaneous treatment by EC. The initial pH was not adjusted and was 5.23 ± 0.37 . All experiments were conducted in duplicate. The aliquots were taken periodically, filtered through a $0.45\text{-}\mu\text{m}$ cellulose-acetate membrane filter, and acidified with a 1% HNO_3 solution for analysis. The pH was measured with a pH meter (Orion 5 star, Thermo), and the heavy metal concentration was analyzed using inductively coupled plasma (OPTIMA 5300 DV, Perkin-Elmer). All reagents in this study were purchased from Sigma-Aldrich.

2.2. Sludge characterization

The sludge resulting from EC using Fe and Al electrodes, at 12.5 A m^{-2} and an initial heavy metal concentration of 50 mg L^{-1} , was collected periodically to investigate the electrostatic characteristics of Fe and Al sludge. The sludge was dewatered by filtration with a $0.45\text{-}\mu\text{m}$ cellulose-acetate membrane filter, washed with DIW, and freeze-dried (FDB-5,503, OPERON). The zeta potential of the sludge was

measured with a zeta potential analyzer (ZetaPlus, Brookhaven). For further characterization of sludge, flocs were taken after a 15-min EC reaction using Fe electrodes at 12.5 A m^{-2} with initial heavy metal concentrations of 100, 200, and 400 mg L^{-1} . A high initial heavy metal concentration was adopted to increase the heavy metal amount in the sludge because the analysis can be hindered by a higher fraction of Fe compounds. The reaction time of 15 min was determined because the heavy metal content of the floc was at its maximum at this time, based on the removed heavy metal amount during EC experiments performed as described in Section 2.1, and on the electrically dissolved Fe amount calculated with Faraday's law. The sludge was dewatered, washed, and freeze-dried as described above. The dried sludge was studied by XRD (M18XHF-SRA, MAC Science), and the results were compared with the heavy metal and Fe speciation using Visual MINTEQ (<http://www.lwr.kth.se/English/OurSoftware/vminteq/#download>). SEM (LEO SUPRA55, Carl Zeiss), TEM (JEM-2100F, JEOL), and EDS (Genesis 2000, EDAX) were used to investigate the microstructure of the sludge.

3. Results and discussion

3.1. Heavy metals removal with different electrode materials

The results provided in Fig. 1(a) show that Fe is better than Al for the removal of Pb(II), Cd(II), and Cu(II), which is in agreement with the findings of previous studies [6,9]. After 15 min of reaction time with an Fe electrode and an Al electrode, Pb(II) removal efficiency was 94.65 and 81.15%, respectively, Cd(II) removal efficiency was 68.36 and 56.18%, respectively, and Cu(II) removal efficiency was 68.75 and 39.21%, respectively. The removal efficiency of the heavy metals reached a plateau after 45 min for both electrodes, and the final removal efficiencies of the heavy metals at 90 min for the Fe and Al electrodes were $98.68 \pm 1.05\%$ and $98.41 \pm 0.18\%$, respectively. The superiority of Fe to Al would be due to the higher adsorption capacity of heavy metals by hydrous ferric oxide than hydrous aluminum oxide [7]. In addition, the amount of Fe(II) released by electrodisolution is greater than Al(III) when the same electrical current is applied, because the electrodisolution amount is inversely proportional to the valance of the metal ion, according to the Faraday's law. This leads to the formation of more Fe(II)/Fe(III) oxides/hydroxides than Al hydroxides [8].

Meanwhile, the maximum heavy metal adsorption capacity of the flocs from EC using Fe electrodes was determined by a separate experiment at 3-h equilibrium and at room temperature. The initial pH and

final pH were 4.6 ± 0.1 and 5.04, respectively. The maximum adsorption capacities for Pb(II), Cd(II), and Cu(II), determined by the Langmuir isotherm, were 5.04, 0.99, and $1.09 \text{ mg g Fe}^{-1}$, respectively. The adsorption capacity was much lower than the removed heavy metals amount per unit mass of Fe generated during EC. This indicates that precipitation and other electrochemical reactions contribute to the removal of heavy metals during EC.

The pH increased as the reaction time increased for all experiments (Fig. 1(b)), due to the OH^- generation and hydrogen evolution at the cathode and due to the oversaturation and release of CO_2 from an aqueous solution under acidic conditions, owing to H_2 bubble disturbance [15]. The pH was higher when an Al electrode was used for the shorter reaction period. However, the pH of the solution electrocoagulated with the Fe electrode exceeded the pH of the solution electrocoagulated with an Al electrode after 60, 30, and 25 min for Pb, Cd, and Cu, respectively. The lower pH for the Al electrodes during the later reaction period can be attributed to hydrolysis of Al species. Various monomeric and polymeric Al species, such as $[\text{Al}_2(\text{OH})_2]^{4+}$, $[\text{Al}_3(\text{OH})_4]^{5+}$, $[\text{Al}_6(\text{OH})_{15}]^{3+}$, $[\text{Al}_7(\text{OH})_{17}]^{4+}$, $[\text{Al}_8(\text{OH})_{20}]^{4+}$, $[\text{Al}_{13}\text{O}_4(\text{OH})_{24}]^{7+}$, and $[\text{Al}_{13}(\text{OH})_{34}]^{5+}$, are generated by the hydrolysis under alkaline pH condition during the later period of EC, which makes the vicinity of an anode become acidic [16].

The dissolved Fe and Al concentrations during EC were analyzed to investigate the possibility of secondary pollution. The results showed that the concentration of Fe was higher than that of Al; however, the concentrations of both Fe and Al in the aqueous phase were negligible after 30 min (Fig. 1(c)). It is believed that the results are due to the higher optimum pH of Fe(II) than Al(III) for precipitate (oxide/hydroxide) formation. $\text{Al}(\text{OH})_3$ is formed at pH levels higher than 5.5 [17]. The pH during Pb(II) removal was higher than 5.5 for the whole reaction period when Al electrodes were used. When Fe electrodes are used, Fe(II) is released as a result of the electrodisolution of Fe^0 and is oxidized to Fe(III) in the presence of dissolved oxygen [18]. This results in a change in the color of the sludge, from green to yellow, which was also observed in this research. Fe(II) hydroxide and Fe(III) hydroxide begin to form at pH values of around 7 and 2, respectively, according to the pC–pH diagrams [17], while the pH was 5.20–6.03 during the first 30 min of reaction time. Therefore, dissolved Fe(II) is dominant in the early stage of EC, where the pH is below 7 (Fig.1(b)). This can lead to the increase in the dissolved Fe amount in the solution.

Fig. 1(d) shows the zeta potential of the sludge during EC. In the absence of heavy metals, the Fe

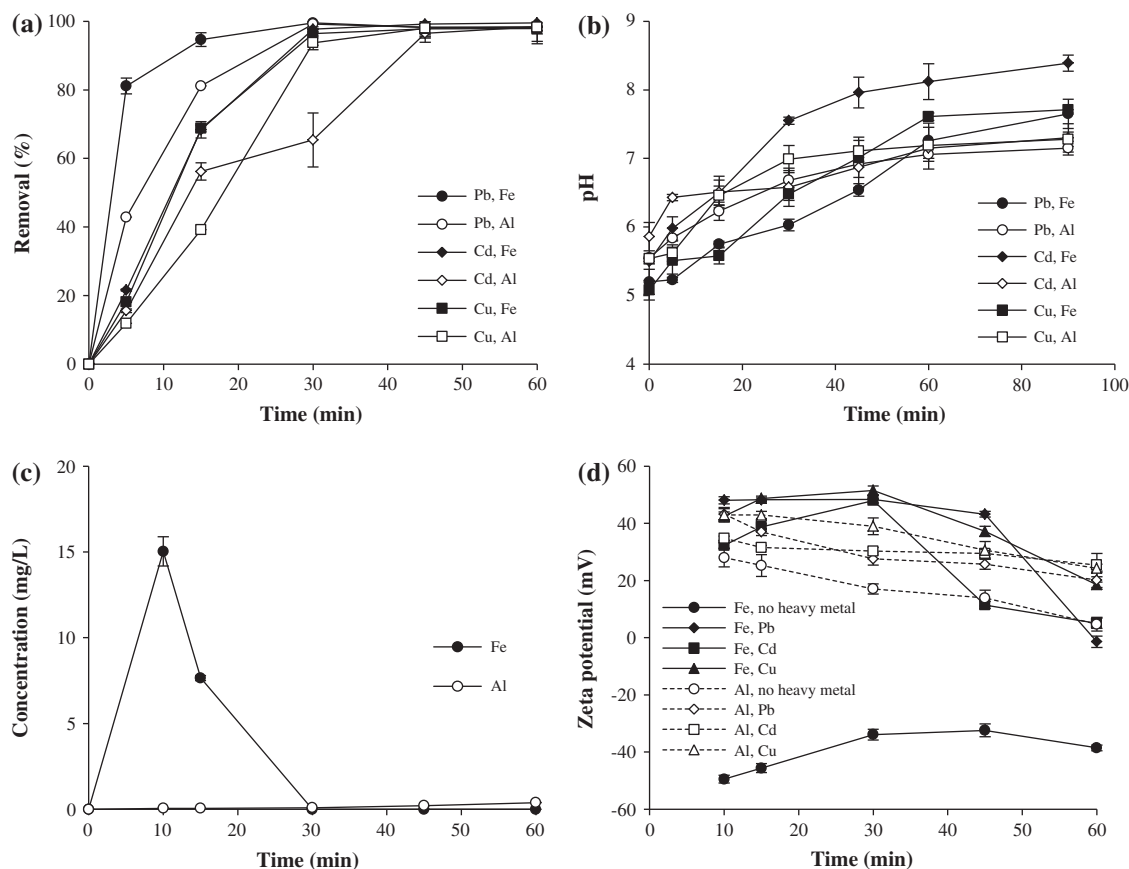


Fig. 1. Time course for (a) heavy metal removal efficiency, (b) pH, (c) dissolved Fe and Al concentration, and (d) zeta potential during EC using different electrodes. Initial heavy metal concentration, 50 mg L^{-1} ; current density, 12.5 A m^{-2} ; background electrolyte, $1 \text{ g L}^{-1} \text{ NaCl}$; electrode area, $25 \times 100 \text{ cm}^2$; electrode distance, 4 mm.

sludge was negative and Al sludge was positive throughout the reaction time of 60 min. The pH increased from 5.61 to 6.06 and from 5.50 to 8.9 when Fe and Al electrodes were used, respectively. The results in Fig. 1(d) suggest that Fe sludge is negatively charged, indicating that an Fe electrode is favorable for cation attraction. Moreover, the dominant species of Fe sludge is Fe oxide, whereas Al(III) forms monomeric and polymeric hydroxides. The oxide surface has a negative charge at higher pH values, which can promote cation attraction [19]. In addition, it can be thought that Al sludge is positively charged, indicating that an Al electrode is more favorable than Fe for the attraction of negatively charged compounds and small particles. It has been reported that Al is better than Fe for the removal of particulate matter, such as algae, and anions, such as phosphate [12,20,21].

When Fe electrodes were used, the zeta potential of the sludge from the EC of Cd(II) and Cu(II) increased, whereas the sludge from the EC of Pb(II) showed a slight decrease, during the first 30 min of reaction time. However, the zeta potential decreased

notably for all heavy metals after 30 min, when Pb(II), Cd(II), and Cu(II) were almost completely removed. It is believed that the increase of zeta potential is due to the consumption of OH^- by forming Fe and heavy metal precipitates and due to the adsorption of heavy metal cations by the sludge, whereas the decrease of zeta potential is due to the accumulation of an excessive amount of OH^- [22]. Meanwhile, the zeta potential of the sludge was positive throughout the reaction time and decreased continuously due to OH^- accumulation, when Al electrodes were used. The positive charge of the Al sludge could be attributed to the pH during EC (Fig. 1(b)), which was lower than the point of zero charge of the Al sludge, which is around 8 [23].

3.2. Effect of current density, initial heavy metal concentration, and coexisting heavy metals on EC by Fe electrodes

The effects of the current density are essential to the study of EC because it is an operational parameter

that can be controlled to change the rate of anode dissolution and metal hydroxide formation on the cathode within an EC cell [8]. In addition, initial heavy metal concentrations should be considered to in establishing optimal EC conditions for the treatment of wastewater under various conditions. Fig. 2 presents the removal efficiency of heavy metals at a reaction time of 15 min at various initial concentrations and current density. After 60 min of EC, most of the heavy metals were removed, regardless of the reaction conditions in this study.

As shown in Fig. 2, heavy metal removal efficiency increased as the current density increased, therefore the coagulant amount increased, and as the initial concentration decreased. This indicates that heavy metal removal efficiency increases as the ratio of the coagulant amount to heavy metal amount increases. The pH increased more rapidly as the current density increased since more OH^- is generated from the cathode, whereas the pH increase was slower when the initial heavy metal concentration increased since more OH^- is consumed by the abundant heavy metals (data

not shown). Meanwhile, Pb(II) was the least sensitive and Cd(II) was the most sensitive to the current density and initial concentration. For Cu(II), the removal efficiency at 15 min increased as the current density increased. The influence of the initial concentration on Cu(II) removal was not significant when it was 10 and 50 mg L^{-1} . However, the initial concentration affected Cu(II) removal significantly when the initial concentration was 100 mg L^{-1} . This indicates that Pb(II) removal is less sensitive to the floc amount, Cd(II) removal is very sensitive to the Cd(II) amount per unit amount of flocs, and Cu(II) removal is mainly affected by the electric current applied. Therefore, it can be suggested that Pb(II), Cd(II), and Cu(II) removal is induced primarily by precipitation, adsorption onto flocs, and by the electrochemical reaction, respectively.

Fig. 3(a) shows that the removal of each heavy metal was more greatly suppressed when Pb(II), Cd(II), and Cu(II) were simultaneously treated than when they were treated individually. In particular, Cd(II) removal was greatly suppressed, while Cu(II)

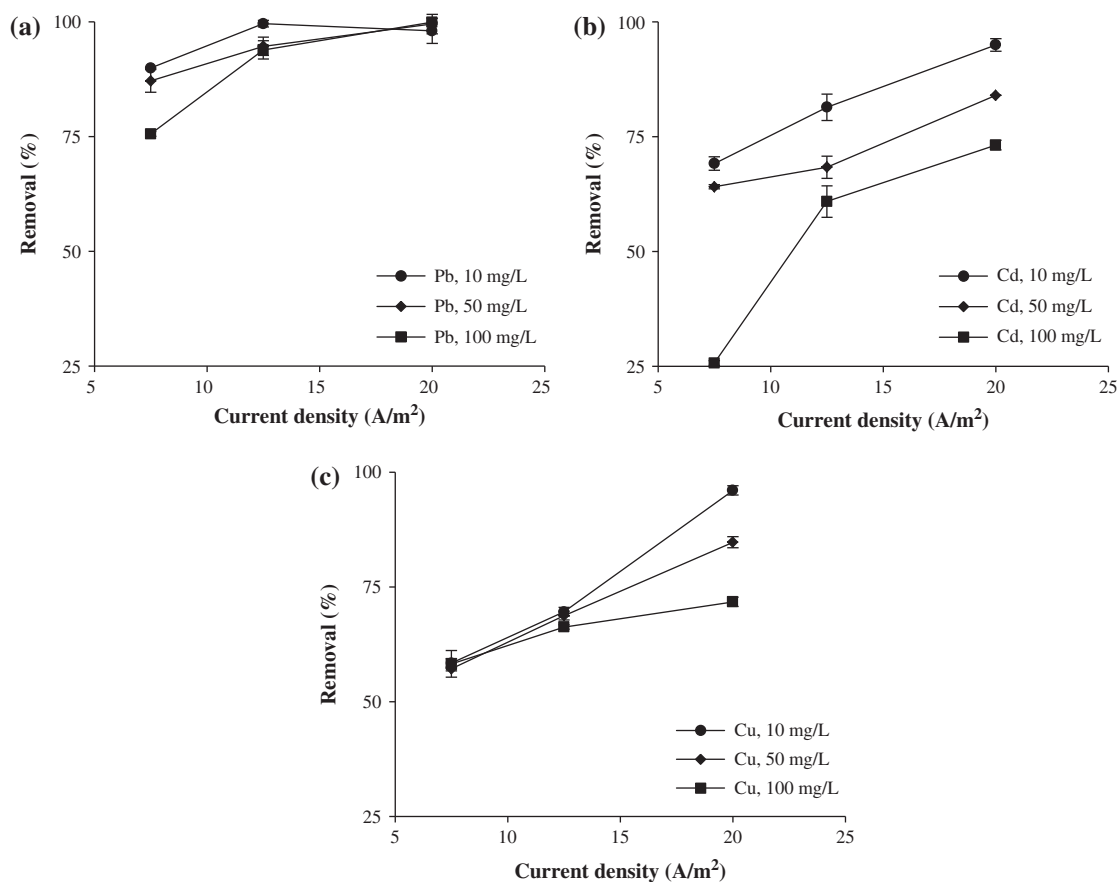


Fig. 2. The removal efficiency of (a) Pb, (b) Cd, and (c) Cu at 15 min of EC time, at various initial concentrations and current density.

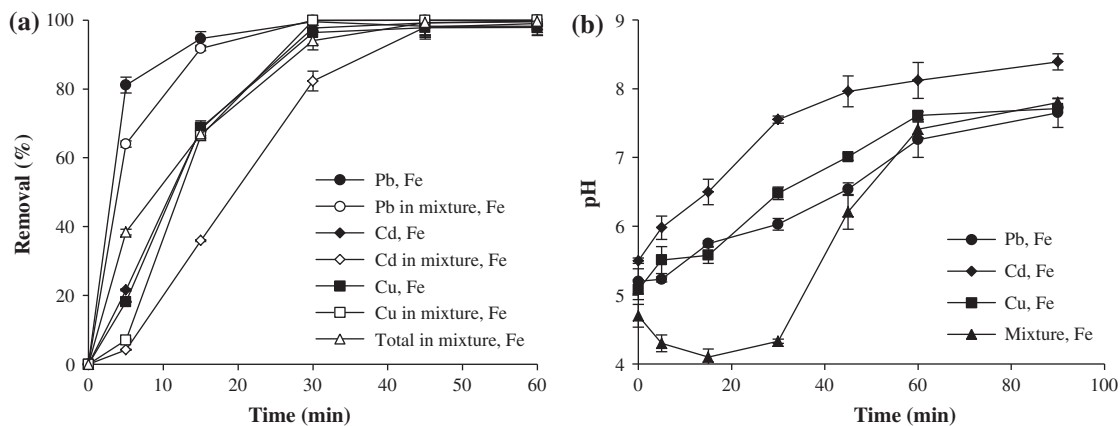


Fig. 3. Time course for (a) heavy metal removal efficiency and (b) pH during EC when Pb, Cd, or Cu exists independently and when all of them exist as a mixture. Initial heavy metal concentration, 50 mg L^{-1} ; current density, 12.5 A m^{-2} ; background electrolyte, 1 g L^{-1} NaCl; electrode area, $25 \times 100 \text{ cm}^2$; electrodes distance, 4 mm; electrode material, Fe.

removal did not show a notable change. It is thought that the suppression is attributed to the decrease of available sludge and OH^- per unit mass of heavy metals. The total heavy metals concentration in the mixture solution was three times higher than that in a single metal solution; therefore, the heavy metals would compete for OH^- and/or sludge for precipitation and/or adsorption. The removal efficiencies of Pb (II), Cd(II), Cu(II), and the combined heavy metals increased as the initial heavy metals concentration decreased and as the current density increased, also indicating that the floc amount plays an important role in EC treatment of heavy metals. Meanwhile, the great suppression of Cd(II) removal indicates a lower affinity of Cd(II) toward the Fe oxides/hydroxides, which are generated by EC using Fe electrodes, than the affinities demonstrated by Pb(II) and Cu(II) [24].

Distinct from the results of the single heavy metal experiments, the pH decreased during the first 15 min of reaction, probably due to the excessive OH^- consumption by abundant heavy metals. The lower pH would hinder the metal precipitation, which adversely affects the removal of heavy metals. The pH increased rapidly thereafter due to the OH^- accumulation, since the available heavy metal ions, which consume OH^- to form metal hydroxides precipitates, were almost completely removed [22].

Meanwhile, the Pb(II) removal rate was the highest, rather than that for Cu(II) or Cd(II), for all experiments in this study, regardless of the heavy metal concentration, current density, and the presence of other heavy metals. It seems that this can be attributed to the first ionization energy, electronegativity, and hydrated radius. The ionization energies of Pb(II), Cu(II), and Cd(II) are 7.417, 7.726, and 8.994 eV,

respectively [25], the electronegativities are 2.33, 1.90, and 1.69, respectively [25], and the hydrated radii are 0.187, 0.21, and 0.23 nm, respectively [26]. A metal with a lower ionization energy, a higher electronegativity, and a smaller hydrated radius are favorable for adsorption to a solid in aqueous solution because the metal requires a smaller energy to remove the outermost electron, attracts more electrons, and exerts stronger coulombic forces of attraction [27].

3.3. XRD analysis of the sludge generated during EC with Fe electrodes.

The XRD patterns in Fig. 4 show that magnetite (Fe_3O_4) is dominant in the sludge generated without heavy metals. It was also reported in a previous study that hematite, maghemite, magnetite, lepidocrocite, and goethite were identified in the by-products of As treatment using EC with an Al-Fe electrodes pair [28]. However, the XRD patterns were different when heavy metals were present. No characteristic peak was found in the XRD patterns of the sludge generated at initial Pb(II) or Cd(II) concentrations of 100 mg L^{-1} , indicating the formation of an amorphous structure. In addition, the peaks corresponding to $\beta\text{-Fe}_2\text{O}_3$ and $\text{Pb}(\text{OH})\text{Cl}$ were observed for the sludge generated at initial Pb(II) concentration of 200 mg L^{-1} , and only $\text{Pb}(\text{OH})\text{Cl}$ was identified at an initial Pb(II) concentration of 400 mg L^{-1} (Fig. 4(a)). For the sludge from the EC treatment of Cd(II), the corresponding peaks to $\text{Fe}_2\text{O}_3 \cdot \text{H}_2\text{O}$ and FeOOH were identified and $\text{Fe}_2\text{O}_3 \cdot \text{H}_2\text{O}$ and $\beta\text{-Cd}_2(\text{OH})_3\text{Cl}$ were identified at initial Cd(II) concentrations of 200 and 400 mg L^{-1} , respectively (Fig. 4(b)). For the sludge from the EC treatment of Cu(II), the corresponding peaks to

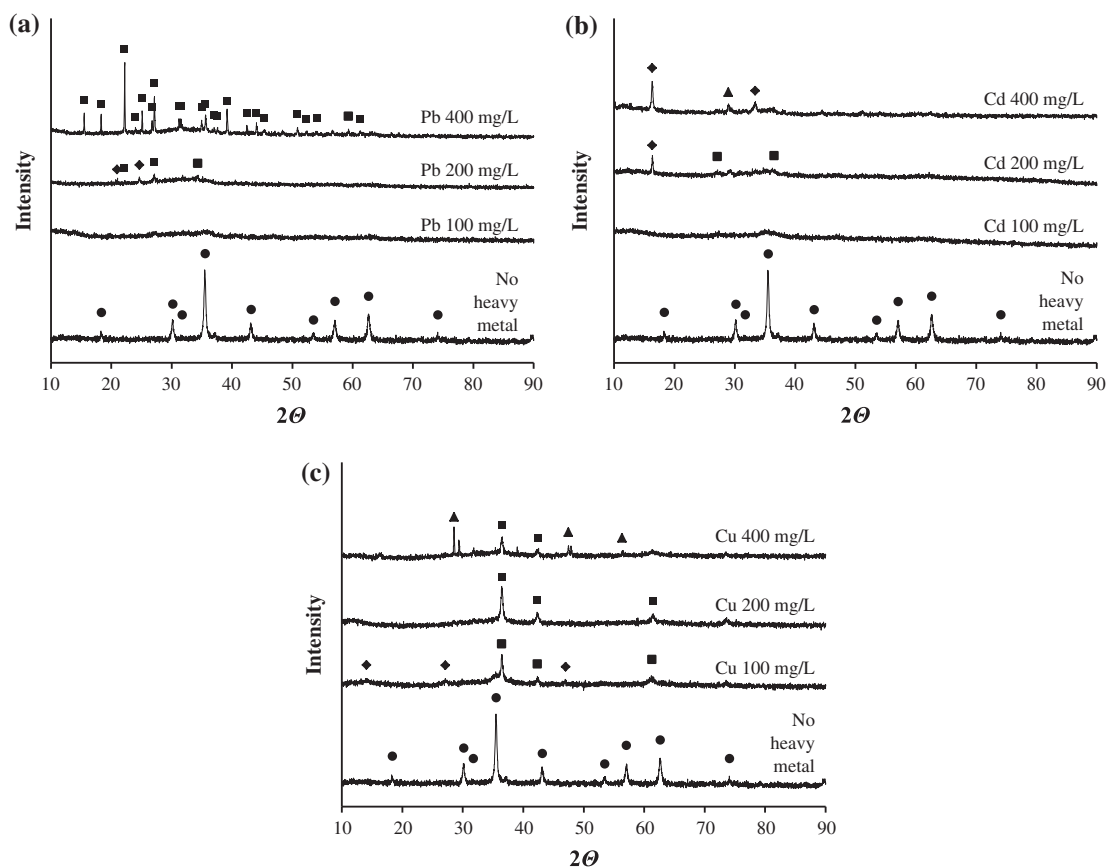


Fig. 4. XRD patterns of (a) Pb (● Fe_3O_4 (magnetite), ◆ $\beta\text{-Fe}_2\text{O}_3$, ■ $\text{Pb}(\text{OH})\text{Cl}$), (b) Cd (● Fe_3O_4 (magnetite), ◆ $\text{Fe}_2\text{O}_3\cdot\text{H}_2\text{O}$, ■ FeOOH (lepidocrocite), ▲ $\beta\text{-Cd}_2(\text{OH})_3\text{Cl}$), and (c) Cu (● Fe_3O_4 (magnetite), ◆ FeOOH (lepidocrocite), ■ Cu_2O , ▲ CuCl) sludge generated by EC at different initial heavy metal concentrations. Current density, 12.5 A m^{-2} ; background electrolyte, 1 g L^{-1} NaCl; electrode area, $25 \times 100 \text{ cm}^2$; electrode distance, 4 mm; electrode material, Fe; reaction time, 15 min.

FeOOH and Cu_2O were identified, Cu_2O was identified, and Cu_2O and CuCl (nantokite) were identified at initial $\text{Cu}(\text{II})$ concentrations of 100, 200, and 400 mg L^{-1} , respectively (Fig. 4(c)). The chlorinated metal species are commonly found in the EC sludge of $\text{Pb}(\text{II})$, $\text{Cd}(\text{II})$, and $\text{Cu}(\text{II})$, indicating that the chloride from NaCl contributed to the heavy metal precipitation.

The heavy metal species identified by XRD analysis can be formed in a system without electricity. $\text{Pb}(\text{OH})\text{Cl}$ can be generated by the hydration of PbCl_2 [29]. $\alpha\text{-Cd}_2(\text{OH})_3\text{Cl}$ and $\beta\text{-Cd}_2(\text{OH})_3\text{Cl}$ can be generated from $\gamma\text{-Cd}(\text{OH})_2$ at 343 K [30]. Cu_2O can be electrodeposited by the reduction of an alkaline aqueous solution of cupric lactate, according to the reaction proposed by Zhou et al. [31], and CuCl (nantokite) is formed by copper corrosion under reductive conditions [32]. Therefore, it can be suggested that Cu_2O was formed in the vicinity of the anode, where $\text{O}_{2(\text{g})}$ is generated by the electrolysis of water, whereas CuCl was formed by the direct reduction of $\text{Cu}(\text{II})$ at the cathode and/or by the reduction through $\text{Fe}(\text{II})$ electrodisolved from the anode. This indicates that

$\text{Cu}(\text{II})$ removal by EC is greatly influenced by the applied current. It also provides an explanation about the observation in Fig. 2(c) that $\text{Cu}(\text{II})$ removal by EC is dependent on the current density, rather than the initial $\text{Cu}(\text{II})$ concentration.

Meanwhile, the chemical equilibrium calculations, obtained by using Visual MINTEQ, indicated that $\alpha\text{-Fe}_2\text{O}_3$ and $\text{Fe}(\text{OH})_2\text{Cl}_{3(\text{s})}$ exist in the sludge from the EC of $\text{Pb}(\text{II})$, $\text{Cd}(\text{II})$, or $\text{Cu}(\text{II})$ under pH values of less than 7.0. No heavy metal precipitate was anticipated by Visual MINTEQ. Therefore, it is evident that many electrochemical and chemical processes, other than chemical equilibration, are involved during the EC process.

3.4. SEM and TEM analysis of the sludge generated during EC with Fe electrodes.

SEM images, TEM images, and their corresponding elemental ($\text{Pb}(\text{II})$, $\text{Cd}(\text{II})$, and $\text{Cu}(\text{II})$) mapping results of EC sludge, generated at an initial heavy metal concentration of 200 mg L^{-1} , are presented in Fig. 5.

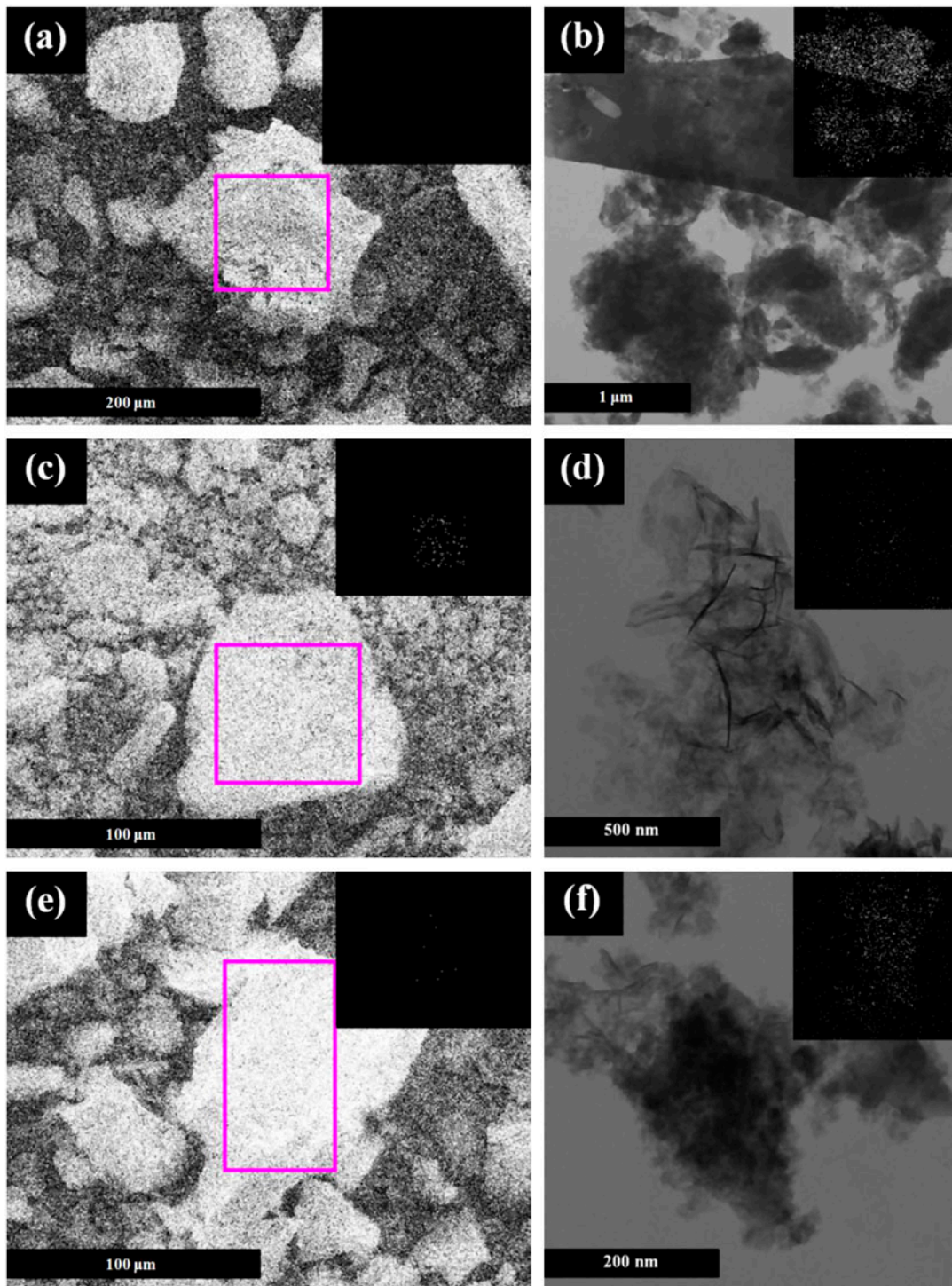


Fig. 5. (a) SEM image and (b) TEM image of the sludge from Pb removal by EC (insets are Pb elemental mapping); (c) SEM image and (d) TEM image of the sludge from Cd removal by EC (insets are Cd elemental mapping); (e) SEM image and (f) TEM image of the sludge from Cu removal by EC (insets are Cu elemental mapping). Initial heavy metals concentration, 200 mg L^{-1} ; current density, 12.5 A m^{-2} ; background electrolyte, $1 \text{ g L}^{-1} \text{ NaCl}$; electrode area, $25 \times 100 \text{ cm}^2$; electrode distance, 4 mm; electrode material, Fe; reaction time, 15 min.

Table 1
Elemental composition of EC sludge by EDS analysis (Fe electrode; initial Pb(II), Cd(II), or Cu(II) concentration, 200 mg L⁻¹; current density, 12.5 A m⁻²; reaction time, 15 min)

	Pb						Cd						Cu					
	SEM			TEM			SEM			TEM			SEM			TEM		
	Weight %	Atomic %		Weight %	Atomic %		Weight %	Atomic %		Weight %	Atomic %		Weight %	Atomic %		Weight %	Atomic %	
O K	33.77	49.09		11.88	41.05		69.23	86.41		18.24	46.15		68.08	84.51		32.96	63.16	
Na K	33.68	34.07		0.90	2.18		5.03	4.37					5.75	4.96				
Cl K	22.94	15.05		2.26	3.51		6.45	3.64		1.20	1.36		6.47	3.63		6.40	5.53	
Fe K	2.35	0.98		20.19	19.98		11.98	4.28		25.07	18.18		17.34	6.17		30.77	16.89	
Pb M	7.26	0.81		38.22	10.20		-	-		-	-		-	-		-	-	
Cd L	-	-		-	-		7.31	1.30		3.79	1.36		-	-		-	-	
Cu K	-	-		26.55	23.09		-	-		51.70	32.94		2.36	0.74		29.87	14.42	

The SEM images of Pb(II), Cd(II), and Cu(II) sludge show irregularly shaped particles of various sizes, without any notable difference between them (Fig. 4(a),(c),(e)). The TEM image of Pb(II) sludge shows randomly aggregated irregular particles, possibly hematite, maghemite, magnetite, or ferrihydrite [33,34] (Fig. 5(b)), consistent with the XRD results (Fig. 4(a)). However, thread-like structures are observed in the TEM image of Cd(II) sludge (Fig. 5(d)), suggesting the presence of goethite (α -FeOOH) and/or lepidocrocite (γ -FeOOH) [34,35], consistent with the XRD results (Fig. 4(b)). Irregular particles are dominant for the Cu(II) sludge, but some thread-like structures are also shown (Fig. 5(f)).

Elemental mapping results show that more Pb(II) and Cu(II) are found in TEM images than SEM images of Pb(II) and Cu(II) sludge (Fig. 5(a),(b),(e),(f)). Furthermore, Pb(II) is hardly found in the SEM image. The EDS analysis, presented in Table 1, also shows that both the weight fraction of Pb(II) or Cu(II) from the total weight of all the atoms in the sample (weight %) and the fraction of the number of the atoms of Pb(II) or Cu(II) from the total number of the atoms in the sample (atomic %) were greater in TEM analysis than in SEM analysis. This indicates that Pb(II) and Cu(II), especially Pb(II), were removed by coprecipitation by occlusion, where they were physically trapped inside the floc [36]. However, significant amounts of Cd(II) were observed in both the SEM and TEM images (Fig. 5(c),(d)), suggesting that Cd(II) was removed mostly by the adsorption onto the flocs as a cation. This is supported by the faster pH increase and higher pH during EC of Cd(II) than was the case of Pb(II) or Cu(II), as shown in Fig. 1(b), indicating less OH⁻ consumption by Cd(II). These results are in agreement with a former study, which suggested the possibility that the removal mechanism of Cd(II) could be different from that of Pb(II) and Cu(II) [9]. Christophi et al. [37], in a study about Pb(II), Cd(II), and Cu(II) adsorption on goethite, also found that Cd exhibits the greatest polarizability of the three metals and forms the least amount of hydroxo species.

4. Conclusions

EC was found to be highly efficient for the removal of heavy metals. For the EC treatment of heavy metals, Fe electrodes were better than Al electrodes, showing both a higher removal efficiency and rate. This is because the Fe flocs are negatively charged, whereas Al flocs are positively charged and because Al hydroxide forms monomeric and polymeric Al species as the reaction time increases. The dissolved Fe concentration was high in the early

period of the reaction when Fe electrodes were used, but it decreased rapidly to be negligible.

The removal efficiency and rate of heavy metals increased as the current density increased and as the initial concentration decreased, indicating that removal of heavy metals by EC is closely related to the heavy metal amount per unit amount of flocs. When Pb, Cd, and Cu exist together, each heavy metal removal was suppressed, and the order of removal efficiency was $Pb(II) > Cu(II) > Cd(II)$, as in the order of ionization energy, electronegativity, and hydrated radius. Among the heavy metals investigated, Pb(II) showed the highest removal efficiency and the least sensitivity to the current density and initial concentration, whereas Cd showed the highest sensitivity. Cu removal was strongly dependent on the current density, rather than initial concentration. This indicates, along with the XRD analysis results, that Cu precipitation is influenced by the electric current, rather than OH^- .

XRD analysis and chemical equilibrium analysis of the EC sludge indicate that various electrochemical and chemical reactions were involved during EC. The existence of magnetite, lepidocrocite, $Pb(OH)Cl$, β - $Cd_2(OH)_3Cl$, Cu_2O , and $CuCl$ was identified by the XRD patterns. In addition, it is suggested that chloride from background electrolyte contributes significantly to heavy metal precipitation, as evidenced by the existence of chlorinated metals in the solid phase. The encapsulation of Pb(II) and Cu(II) was evidenced by the SEM and TEM images, indicating that precipitation plays an important role in Pb(II) and Cu(II) removal. The XRD, SEM, and TEM analysis results of Cd(II) sludge showed that Cd(II) removal is achieved by adsorption, rather than precipitation.

Acknowledgement

This subject is supported by Korea Ministry of Environment as "The GAIA Project".

References

- [1] F. Fu, Q. Wang, Removal of heavy metal ions from wastewaters: A review, *J. Environ. Manage.* 92(3) (2011) 407–418.
- [2] J.J. Mortvedt, Heavy metal contaminants in inorganic and organic fertilizers, *Fert. Res.* 43(1–3) (1996) 55–61.
- [3] E.U. Etim, P.C. Onianwa, Lead contamination of soil in the vicinity of a military shooting range in Ibadan, Nigeria, *Toxicol. Environ. Chem.* 94(5) (2012) 895–905.
- [4] F. Akbal, S. Camci, Comparison of electrocoagulation and chemical coagulation for heavy metal removal, *Chem. Eng. Technol.* 33(10) (2010) 1655–1664.
- [5] B. Al Aji, Y. Yavuz, A.S. Kopalal, Electrocoagulation of heavy metals containing model wastewater using monopolar iron electrodes, *Sep. Purif. Technol.* 86 (2012) 248–254.
- [6] A.K. Yadav, L. Singh, A. Mohanty, S. Satya, T.R. Sreekrishnan, Removal of various pollutants from wastewater by electrocoagulation using iron and aluminium electrode, *Desalin. Water Treat.* 46(1–3) (2012) 352–358.
- [7] P.R. Kumar, S. Chaudhari, K.C. Khilar, S.P. Mahajan, Removal of arsenic from water by Electrocoagulation, *Chemosphere* 55(9) (2004) 1245–1252.
- [8] C.P. Nansu-Njiki, S.R. Tchamango, P.C. Ngom, A. Darchen, E. Ngameni, Mercury(II) removal from water by electrocoagulation using aluminium and iron electrodes, *J. Hazard. Mater.* 168(2–3) (2009) 1430–1436.
- [9] D. Kumarasinghe, L. Pettigrew, L.D. Nghiem, Removal of heavy metals from mining impacted water by an electrocoagulation-ultrafiltration hybrid process, *Desalin. Water Treat.* 11 (2009) 66–72.
- [10] S. Zodi, O. Potier, F. Lapique, J.-P. Leclerc, Treatment of the textile wastewaters by electrocoagulation: Effect of operating parameters on the sludge settling characteristics, *Sep. Purif. Technol.* 69 (2009) 29–36.
- [11] D. Ghernaout, M.W. Naceur, B. Ghernaout, A review of electrocoagulation as a promising coagulation process for improved organic and inorganic matters removal by electrophoresis and electroflotation, *Desalin. Water Treat.* 28(1–3) (2011) 287–320.
- [12] Ş. İrdemez, Y. Sevki Yildiz, V. Tosunoglu, Optimization of phosphate removal from wastewater by electrocoagulation with aluminium plate electrodes, *Sep. Purif. Technol.* 52(2) (2006) 394–401.
- [13] A.K. Golder, A.N. Samanta, S. Ray, Removal of trivalent chromium by electrocoagulation, *Sep. Purif. Technol.* 53 (2007) 33–41.
- [14] N. Drouiche, H. Lounici, M. Drouiche, N. Mameri, N. Ghafour, Removal of fluoride from photovoltaic wastewater by electrocoagulation and products characteristics, *Desalin. Water Treat.* 7(1–3) (2009) 236–241.
- [15] X. Chen, G. Chen, L.Y. Po, Separation of pollutants from restaurant wastewater by electrocoagulation, *Sep. Purif. Technol.* 19(1–2) (2000) 65–76.
- [16] G. Mouedhen, M. Feki, M. De Petris Wery, H.F. Ayedi, Behavior of aluminum electrodes in electrocoagulation process, *J. Hazard. Mater.* 150 (2008) 124–135.
- [17] V.L. Snoeyink, D. Jenkins, *Water Chemistry*, Wiley, New York, 1980.
- [18] Z. Zaroual, M. Azzi, N. Saib, E. Chainet, Contribution to the study of electrocoagulation mechanism in basic textile effluent, *J. Hazard. Mater.* 131(1–3) (2006) 73–78.
- [19] M. Kobya, E. Demirbas, A. Dedeli, M.T. Sensoy, Treatment of rinse water from zinc phosphate coating by batch and continuous electrocoagulation processes, *J. Hazard. Mater.* 173(1–3) (2010) 326–334.
- [20] Ş. İrdemez, N. Demircioglu, Y.S. Yildiz, The effects of pH on phosphate removal from wastewater by electrocoagulation with iron plate electrodes, *J. Hazard. Mater.* B137(2) (2006) 1231–1235.
- [21] S. Gao, J. Yang, J. Tian, F. Ma, G. Tu, M. Du, Electro-coagulation-flotation process for algae removal, *J. Hazard. Mater.* 177 (2010) 336–343.
- [22] J.L. Trompette, H. Vergnes, On the crucial influence of some supporting electrolytes during electrocoagulation in the presence of aluminum electrodes, *J. Hazard. Mater.* 163 (2009) 1282–1288.
- [23] T. Harif, M. Khai, A. Adin, Electrocoagulation versus chemical coagulation: Coagulation/flocculation mechanisms and resulting floc characteristics, *Water Res.* 46(10) (2012) 3177–3188.
- [24] B.-H. Jeon, B.A. Dempsey, W.D. Burgos, R.A. Royer, Sorption kinetics of Fe(II), Zn(II), Co(II), Ni(II), Cd(II), and Fe(II)/Me(II) onto hematite, *Water Res.* 37 (2003) 4135–4142.
- [25] D.R. Lide, (Ed.), *CRC Handbook of Chemistry and Physics*, 84th ed., CRC Press, Boca Raton, FL, 2003.

- [26] X.S. Wang, H.H. Miao, W. He, H.L. Shen, Competitive adsorption of Pb(II), Cu(II), and Cd(II) ions on wheat-residue derived black carbon, *J. Chem. Eng. Data* 56 (2011) 444–449.
- [27] J.K. Mitchell, *Fundamentals of Soil Behavior*, 2nd ed., Wiley, New York, 1993.
- [28] J.A.G. Gomes, P. Daida, M. Kesmez, M. Weir, H. Moreno, J.R. Parga, G. Irwin, H. McWhinney, T. Grady, E. Peterson, D.L. Cocke, Arsenic removal by electrocoagulation using combined Al-Fe electrode system and characterization of products, *J. Hazard. Mater.* 139(2) (2007) 220–231.
- [29] Y. Chen, Q. Wu, R. Yin, Y. Ding, Facile fabrication and optical properties of novel Pb(OH)Cl nanotubes, *J. Nanopart. Res.* 9 (2007) 283–287.
- [30] Y. Cudennec, A. Riou, Y. Gerault, A. Lecerf, Synthesis and crystal structures of Cd(OH)Cl and Cu(OH)Cl and relationship to brucite type, *J. Solid State Chem.* 151 (2000) 308–312.
- [31] Y. Zhou, J.A. Switzer, Electrochemical deposition and microstructure of Copper (I) oxide-films, *Scripta Mater.* 38(11) (1998) 1731–1738.
- [32] M. Dowsett, A. Adriaens, C. Martin, L. Bouchenoire, The use of synchrotron X-rays to observe copper corrosion in real time, *Anal. Chem.* 84(11) (2012) 4866–4872.
- [33] A. Mohapatra, L. Mohapatra, P. Singh, S. Anand, B.K. Mishra, A comparative study on Pb(II), Cd(II), Cu(II), Co(II) adsorption from single and binary aqueous solutions on additive assisted nano-structured goethite, *Int. J. Eng. Sci. Technol.* 2(8) (2010) 89–103.
- [34] M. Usman, K. Hanna, M. Abdelmoula, A. Zegeye, P. Faure, C. Ruby, Formation of green rust via mineralogical transformation of ferric oxides (ferrihydrite, goethite and hematite), *Appl. Clay Sci.* 64 (2012) 38–43.
- [35] Y. Lin, Y. Wei, Y. Sun, Room-temperature synthesis and photocatalytic properties of lepidocrocite by monowavelength visible light irradiation, *J. Mol. Catal. A-Chem.* 353–354 (2012) 67–73.
- [36] D. Harvey, *Modern Analytical Chemistry*, McGraw-Hill, Boston, MA, 2000.
- [37] C.A. Christophi, L. Axe, Competition of Cd Cu and Pb adsorption on goethite, *J. Environ. Eng.-ASCE* 126(1) (2000) 66–74.